

ASSESSMENT OF NANOIRON-METAL ORGANIC FRAMEWORKS AND GALLIC ACID FOR HEAT STRESS TOLERANCE IN WHEAT AT NEW VALLEY

Noura E. Mahmoud

Biochemistry Unit, Department of Genetic Resources, Desert Research Center, Cairo, Egypt

E-mail: saidn58@yahoo.com

The field experiment was carried out at the Agricultural Experimental Station of Desert Research Center, at New Valley Governorate during the winter seasons of 2022-2023 for the assessment of the contribution of nanoiron-metal organic frameworks and gallic acid for heat stress tolerance in two wheat cultivars (Giza 171 and Gemmeiza 12). Nano-organic frameworks of iron metal were synthesized, and through various activation processes and the use of high temperatures, gallic acid was introduced and bound into the nano-organic frameworks. Its synthesis and purity were also confirmed by characterizing it using HR-SEM, XRD, and FTIR. Treatment with nanoiron-metal organic frameworks conjugated with gallic acid (FeM4) contributed to alleviating the negative effects of heat stress on the metabolic products of wheat plants and protected them from adverse effects, and this was consistent with growth and yield. In this context, FeM4 had the best effect on improving the productivity of wheat yield by 4.3 and 5.4 times for Giza 171 and Gemmeiza 12, respectively, compared to the control. The increase in some biochemical constituents and the decrease in some other constituents had a role in alleviation negative effects of heat stress on metabolites and protection against the adverse effects of stress. FeM4 treatment led to an increase in the content of photosynthetic pigments, especially chlorophyll (a) by 1.55 times and chlorophyll (b) by 1.42 times, and a decrease in the content of compatible solutes such as proline by 59% and glycinebetaine by 23%, compared to the control. Likewise, the previous treatment led to an increase in the activity of peroxidase and superoxide dismutase enzymes in both wheat cultivars. In the molecular level (ISSR technique), treating the two wheat cultivars with nanoiron-metal organic frameworks and gallic acid did not lead to any noticeable changes in the genetic material. Applying these recommendations in new desert areas exposed to heat stress conditions could play a role in increasing the productivity of wheat

cultivars (especially Giza 171), and this contributes to reducing the wheat nutritional gap in Egypt.

Keywords: heat stress, Fe-MOFs, compatible solutes, wheat, ISSR

INTRODUCTION

Worldwide, wheat (*Triticum aestivum* L.) is a grass that is extensively farmed for its cereal grain, which is a staple diet. Compared to other crops, wheat is grown on much larger plots of land, with an estimated 545 million acres (220.4 million hectares) in 2014 (Nakai, 2018). Wheat, accounts for about 30% of global grain production and 50% of global grain trade. By 2050, FAO predicted that the world will need an additional 198 million tons of wheat to meet demand, which would require emerging nations to raise wheat production by 77% (Sharma et al., 2015). However, the distribution of temperature anomalies is shifting towards higher temperatures and the number of anomalies is growing. It has already been noted that such an occurrence during the crop-growing season lowers wheat productivity in several parts of the world (Mueller et al., 2015). With over 100 million hectares of wheat farmed worldwide in primarily heat-exposed locations, wheat is severely impacted by heat stress (Braun et al., 2010). Artificial heating assessed 30 wheat crop models at growing season temperatures between 15 and 32°C (Asseng et al., 2015). The findings show that most wheat-growing regions have already seen a decrease in grain yield because of global warming.

There were considerable differences in how medium temperature affected wheat yield. Average yields decreased for the years between 1981 and 2010 and ranged from 1 to 28% across 30 locations worldwide for an increase in temperature of 2°C; this value increased to between 6 and 55% for an increase in temperature of 4°C. The effect of the simulated mean temperature on the decline in wheat yield varied greatly. Additionally, previous study predicts that for every 1-degree Celsius increase in temperature, the world's wheat yield declines by 6%. Temperatures higher than those seen at higher latitudes significantly increased yield variability at low latitudes. A higher reference temperature was to blame for this greater relative loss in yield (Challinor et al., 2014).

Heat stress has numerous effects on plants that affect their growth and development, physiological processes, grain production, and yield (Mondal et al., 2013). One of the key climatic elements that influence wheat growth, development, and yield is temperature. In wheat, high temperatures (>31°C) after anthesis can slow down the pace of grain filling quality, and growth (Chutipajit et al., 2009 and Hasanuzzaman et al., 2013). Near anthesis, high-temperature events can decrease the number of grains per ear and, as a result, the rate of harvesting index, leading in lower grain yields (Almeselmani et al., 2006). High temperature has an effect on all stages of wheat growth,

from seedling through grain filling, but anthesis and the early stages of grain filling are the most vulnerable (Farooq et al., 2011). Wheat yield is strongly affected by heat by altering physical and biochemical processes, such as inhibiting photosynthesis by reducing RuBisCO activity and thus reducing light utilization efficiency. Changes in photosynthesis and metabolic activities lead to the creation of ROS, which oxidizes proteins and cell membranes and damages DNA. Antioxidant enzymes include superoxide dismutase, ascorbate peroxidase, glutathione reductase, and dehydroascorbate reductase aid in ROS detoxification (Mittler, 2002). Other study showed that under heat stress, one protein associated with glucose-1-phosphate adenylyltransferase, which is essential for the production of starch, significantly decreased, potentially lowering grain weight (Halder et al., 2022). Likewise, reduced nitrogen and amino acid metabolism under heat stress is indicated by heat stress-induced ROS generation and its effect on nitrogen metabolism and protein-binding amino acid metabolism (Wang et al., 2015). According to a different study, wheat plants' photosynthesis and translation are negatively impacted by high temperatures. Through the elevated heat-responsive proteins, protein folding was considerably enhanced (Lu et al., 2017). A previous study showed that 1°C increase in temperature during the wheat growing season resulted in 3–10% decrease in wheat output (Ahmed and Hassan, 2011). The basal temperature is 4°C, while the ideal temperature for wheat germination is between 20 and 22°C. A temperature between 25 and 32°C is regarded as fairly high during grain growth, whereas a temperature between 35 and 40°C is regarded as very high (Ullah et al., 2021). Wheat production has recently had to contend with some extremely challenging weather circumstances, particularly heat stress from pre-anthesis to physiological maturity. Therefore, it is insufficient to meet the needs of a growing population.

Metal-organic frameworks (MOFs) have become increasingly important in the field of pesticide eradication (Mahmoud et al., 2022a). With inorganic nodes (such as atoms, clusters, or chains) and organic linkers (such as carboxylates, nitrogenates, or phosphonates), MOFs are thought to be a remarkable family of extremely porous coordination polymers that assemble into multidimensional periodic lattices. There have been MOFs proposed for various socioeconomic (Tan et al., 2022). Iron-based MOFs are particularly interesting for their biocompatibility, as they can serve as a good slow-release source of iron, an important micronutrient for plant growth and survival. It can also be used to deliver various agricultural chemicals, such as binding iron to phosphate and oxalate, forming a core of iron phosphate bound to oxalate, and slow release of N (urea) and P (phosphate) fertilizers through microbial decomposition of oxalate. Later, MOFs were used in slow-release agricultural applications (Bindra et al., 2019 and Mahmoud et al., 2022a). The intriguing properties of MOFs make them promising materials for use in agriculture; among their most significant traits are their adaptable hybrid formulations, which enable a wide range of combinations; additionally, they have large

surface areas and defined pore sizes, as well as exceptional adsorption capacity; additionally, they bear simple functional cavities, in which a particular added some active compounds; and finally, since they have been produced on a large basis, they have simple functional cavities. In the agriculture field, MOFs can be utilized to release agrochemicals under control (Rojas et al., 2022). In addition to being essential for the completion of the plant's growth and development cycle, secondary metabolites (such as phenolic compounds) are also crucial for controlling how plants interact with one another and adapt to their environment, as well as for defense mechanisms against biotic and abiotic stresses (Yang et al., 2018).

A phenolic substance called gallic acid (GA) is good at neutralizing free radicals and preventing the oxidation of lipids. Additionally, it lessens the impacts of numerous abiotic stresses such as osmotic pressure, heavy metals, and refrigeration. Through its capacity to inhibit free radicals, improve water status and photosynthetic capacity, and reduce the negative effects of excessive boron damage by reducing boron uptake or preventing growth inhibition, GA treatments in soybean and tomato resulted in tolerance to cold and heavy metals stress (Yildiztugay et al., 2017 and Farghaly et al., 2021). GA is a capping agent that can be utilized to make nanoparticles with a notable potential to enhance plant performance to enhance colloidal stability and stop nanoparticles aggregation, phenolic compounds are utilized as capping agents (Herrera-Becerra et al., 2010; Venkateswarlu et al., 2013 and Alabdallah et al., 2021).

The goal of the research is to examine how GA encapsulated within Fe-MOFs spray treatments affects wheat plants' (Giza 171 and Gemmeiza 12 cultivars) ability to withstand heat stress. Examining the effect on biochemical parameters and the genetic alterations brought on by nanomaterials spraying.

MATERIALS AND METHODS

1. Preparation of Iron Organic Frameworks

1.1. Chemicals and materials

The analytical quality materials utilized were ferrous chloride (FeCl_2) (99.9%, Aldrich), 2-aminoterephthalic acid (99%, Aldrich), N,N-dimethylformamide (DMF, 99.9%, Aldrich), methanol (PA, Fisher Scientific), ethanol (99.9%, Aldrich), and GA (99.9%, Aldrich).

1.2. Preparation method

Fe-MOFs were made in the following way: In 10 mL of DMF, at room temperature, FeCl_2 (1 mL, 3.38 mmol) and 2-aminoterephthalic acid (1 g, 5.5 mmol) were dissolved. The produced slurry was sealed and heated to 110°C for 24 hours in the oven. The unreacted organic ligand was filtered off, rinsed with DMF to remove it, and then washed once more with methanol to exchange DMF. The finished product was vacuum-stored until used after being dried in an oven at 80°C for 4 hours (Abdelhameed et al., 2019). Using

the mixed linker approach, GA encapsulated within Fe-MOFs were created by first adding varying ratios of GA (20%, 30%, and 40%) from the total precursors to 2-aminoterephthalic acid (1 g, 5.5 mmol) and FeCl₂ (1 mL, 3.38 mmol). At room temperature, all particles were dissolved in 10 mL of DMF, which was then heated for 24 hours at 110°C. To eliminate the unreacted organic ligand, the product was filtered out, washed with DMF multiple times, dried, and stored until it was ready to use.

1.3. Instrument and characterization

Using high-resolution scanning electron microscopy (HRSEM Quanta FEG 250 with field emission gun, FEI Company - Netherlands), the morphological structure of Fe-MOFs and GA encapsulated within Fe-MOFs was examined. Cu K α X-radiation at 40 kV, 50 mA, and $\lambda = 1.5406 \text{ \AA}$ at room temperature was used to analyze the samples for X-ray diffraction (XRD), and diffraction data were collected in steps of $2\theta^\circ$ ranging from 4° to 50° with a step size of 0.02° and scanning rate of 1 second. The samples were also subjected to Fourier Transform Infrared Spectroscopy (FTIR) analysis using a Japanese spectrophotometer, the JASCO FT/IR-4700. With 16 repeated scans, a scanning speed of 2 mm s^{-1} , and a spectra resolution of 4 cm^{-1} , the transmission spectra were obtained in the $4000 - 500 \text{ cm}^{-1}$ range with a 1.0 cm^{-1} interval. Baseline correction and smoothing of the spectral data by 25 points were applied.

2. Field Experiment

2.1. Plant material

Two wheat cultivars, Giza 171 (G 171) and Gemmeiza 12 (Gem 12) were obtained from the Institute of Field Crops at the Agricultural Research Center in Giza, Egypt.

2.2. Cultivation

Field experiment was conducted at the experimental station of the Center for Sustainable Development in New Valley Governorate (heat stress) in southwestern Egypt in the Western Desert, to study the biochemical changes caused by GA encapsulated within iron-organic frameworks on two wheat cultivars. Wheat seeds were cultivated by seed driller in rows in three replicates, 50-cm apart, at a rate of 45 kg fed^{-1} at a depth of 3-5 cm below the soil surface on 15 November during the 2022-2023 seasons. Wheat drip-irrigated obtained at rate of 4 L in an hour for 1/2 hour every 3 days and fertilized regularly by fertilizers. All treatments received 100 kg of phosphate fertilizer 15% (monophosphate) fed^{-1} , 24 kg K fed^{-1} as potassium sulphate and N fertilizer at a rate of 163 kg fed^{-1} urea 46% N. The experiments were designed in a split-plot design with three replicates. Other agricultural practices were applied as recommended for the ordinary bread wheat fields at New Valley in the experimental location at the Center for Sustainable Development. Chemical analysis of soil and water are presented in Table (1) and the results were determined according to Allison and Richards (1954) and

Jackson (1958). The meteorological data of New Valley location are presented in Table (2).

Table (1). Physical and chemical analysis of the experimental soil and underground irrigation water at Center for Sustainable Development in New Valley.

a) Physical analysis of the experimental soil									
Particle size distribution %									
Very coarse sand	Coarse sand	Medium sand	Fine sand	Very fine sand	Silt and clay	Soil texture			
18.51	11.33	10.21	19.06	31.22	9.69	Sandy soil			
b) Chemical analysis of the experimental soil									
EC (dS m ⁻¹)	pH	Cations (meq l ⁻¹)					Anions (meq l ⁻¹)		
		Ca ⁺⁺	Mg ⁺⁺	Na ⁺	K ⁺	CO ₃ ⁻⁻	HCO ₃ ⁻	Cl ⁻	SO ₄ ⁻⁻
1.47	8.1	8.47	2.12	3.12	0.67	Nil	3.61	3.79	7.31
c) Chemical analysis of irrigation water									
EC (dS m ⁻¹)	pH	Cations (meq l ⁻¹)					Anions (meq l ⁻¹)		
		Ca ⁺⁺	Mg ⁺⁺	Na ⁺	K ⁺	CO ₃ ⁻⁻	HCO ₃ ⁻	Cl ⁻	SO ₄ ⁻⁻
0.48	7.1	1.27	0.60	2.48	0.63	Nil	3.34	1.22	0.24

Table (2). Meteorological data at Kharga, New Valley, Egypt, from November 2022 to May 2023.

Months	Parameters						
	Temp. (°C)	Max. Temp. (°C)	Min. Temp. (°C)	RH (%)	Rain (mm)	Wind speed (mph)	Sunshine (h)
November	20.59	27.47	13.70	47	0.00	14.20	9.70
December	17.33	24.06	10.61	51	0.10	17.00	8.90
January	15.55	23.00	8.10	52	0.40	13.10	9.30
February	14.78	21.86	7.71	45	0.40	14.00	9.80
March	21.17	29.00	13.35	38	0.60	14.90	9.60
April	25.05	33.10	17.00	29	0.40	15.30	10.20
May	28.91	36.42	21.39	27	0.20	15.60	10.90

Abbreviations: Temp.: temperature, Max.: maximum, Min.: minimum, RH: relative humidity, mph: miles per hour

3. Gallic Acid Encapsulated Within Iron-Organic Frameworks Treatments

Treatments for the investigation included the following: GA at a concentration of 100 µg mL⁻¹; nanoiron-organic frameworks (FeM1) at concentration of 20 µg mL⁻¹, and 20%, 30%, and 40% of GA encapsulated within iron-organic frameworks (FeM2, FeM3, and FeM4) at a concentration of 20 µg mL⁻¹.

Each treatment was sprayed on plants at a rate of 400 liter fed⁻¹ after 20 and 40 days from sowing. Tween 20 (0.05%) was mixed with each treatment as a wetting agent.

Sampling

Two plant samples were taken randomly from each treatment during the experiment of the season as follows: Firstly, fresh plant samples were

collected 50 days after sowing. Fresh samples were tested for photosynthetic pigments, antioxidant enzymes, electrophoretic pattern of proteins, free proline and inter-sample sequence repeat (ISSR- DNA). Then, samples were heated to constant weight in the oven at 65°C representing dry weight. Dry leaves were ground to fine powder and tested for soluble protein and glycinebetaine. Secondary, samples represented by seeds and straw yield, was taken after harvesting.

3. Biochemical Analysis

3.1. Photosynthetic pigments

Chlorophyll a, b and carotenoids were extracted by 85% acetone from fresh wheat leaves and determined spectrometrically. The concentration of chlorophyll a, b and carotenoids were calculated employing Wettstein's formula, and the final concentration of pigments were then expressed in mg g⁻¹ fresh weight of leaves (Wettstein, 1957).

3.2. Free proline

Acid-ninhydrin was prepared by warming 1.25 g ninhydrin in 30 mL glacial acetic acid and 20 mL 6 M phosphoric acid, with agitation, until dissolved. Approximately 0.5 g of fresh wheat leaves was homogenized in 10 mL of 3% aqueous sulfosalicylic acid and the homogenate was filtered through Whatman filter paper. Two mL of filtrate were reacted with 2 mL acid-ninhydrin and 2 mL of glacial acetic acid in a test tube for 1 h at 100°C, and the reaction terminated in an ice bath. The reaction mixture was extracted with 4 mL toluene, mixed vigorously with a test tube stirrer for 15-20 seconds. The chromophore containing toluene was aspirated from the aqueous phase, and the absorbance was read at 520 nm using toluene as a blank. The proline concentration was determined from a standard curve and calculated on a fresh weight basis as follows:

$$[(\mu\text{g proline mL}^{-1} \times \text{mL toluene}) / 115.5 \mu\text{g } \mu\text{mole}^{-1}] / [(\text{g sample})/5] = \mu\text{moles proline/g fresh weight of wheat (Bates et al., 1973).}$$

3.3. Glycinebetaine

Dried finely-ground wheat leaves (0.5 g), was mechanically shaken with 20 mL of H₂O for 24 h at 25°C. The samples were then filtered and diluted 1: 1 with 2 N H₂SO₄ then cooled in ice water for 1 h in a centrifuge tube and 0.5 mL of aliquots were added to 200 μL of cold KI-I₂ reagent, prepared by dissolving 15.7 g of iodine and 20 g of KI in 100 mL water was added and the reactants were gently stirred with a vortex mixer. The tubes were stored at 0-4°C for 16 h and then centrifuged at 10,000 rpm for 15 min at 0°C. The supernatant was carefully aspirated with a fine tipped glass tube. The periodide crystals were dissolved in 9.0 mL of 1,2-dichloroethane (reagent grade). Vigorous vortex mixing was frequently required to affect complete solution in the developing solvent. After 2-2.5 h, the absorbance was measured at 365 nm with a spectrophotometer. Reference standards of glycinebetaine were prepared in 1 N H₂SO₄. The concentration of

glycinebetaine was calculated according to standard curve (Grieve and Grattan, 1983).

3.4. Peroxidase

About 0.5 g of wheat fresh leaves was homogenized with 5 mL of 0.05 M sodium phosphate buffer pH, 7.0. The homogenate was centrifuged at 12,000 rpm at 4°C for 15 min and the supernatant representing the crude enzyme source was preserved at -20°C until being used. Peroxidase was determined by using the *O*-dianisidine method according to the Worthington Biochemical Corp (Worthington, 2011). To 1.5 mL of 0.01 M phosphate buffer (pH, 6.0), 0.01 mL of 1% *O*-dianisidine (1% in absolute methanol) was added and mixed; 0.1 mL of the enzyme was added and mixed. Then 0.1 mL of 0.3% H₂O₂ was added; after mixing, the increase in absorbance was recorded at 460 nm for 3 min by spectrophotometer as $\Delta \text{Abs } 460 / \text{fresh weight} / 3 \text{ min}$.

3.5. Superoxide dismutase isozyme

General protocols for measuring superoxide dismutase (SOD) antioxidant enzyme activity are identified by the Native PAGE protocol (Weydert and Cullen, 2010), which provides the number of bands and their activities. The SODs transform superoxide radicals into hydrogen peroxide and molecular oxygen oxide. SODs were isolated and separated from wheat fresh leaves according to Weydert and Cullen protocol (Weydert and Cullen, 2010).

3.6. Proteins electrophoretic pattern

Half a gram of fresh wheat leaves was added to 400 mL of protein extraction buffer, which contained 6 mL Tris buffer pH 8.8, 0.8 mL 0.25M EDTA, 40 mL 10% SDS + 40 μL β -mercaptoethanol, and then completed to 100 mL with distilled water. In a chilled centrifuge, homogenized materials were spun for 10 min at 4°C at 13,000 rpm. In order to run on a polyacrylamide gel, the crude proteins were extracted as supernatant, transferred to a fresh Eppendorf tube, and kept at 2°C (Steel and Torrie, 1980). SDS-PAGE (Bio-Rad, Model 600, UK) electrophoresis was carried out using a 15% polyacrylamide gel. Using a standard molecular weight protein, the molecular weight of the solute proteins was calculated.

4. Molecular Marker (ISSR-PCR Technique)

4.1. Isolation of plant DNA

Following treatments with nanoparticles, genomic DNA from two wheat cultivars was extracted from 50-day-old seedlings using the CTAB extraction technique described by Doyle and Doyle (1987). Six markers altogether were chosen for the investigation.

4.2. Data analysis

The informativeness of each marker was evaluated using marker polymorphism, and the PIC for each marker was determined using the formula provided by Anderson et al. (1993). By computing the similarity coefficient

(Jaccard, 1908) for pair-wise comparisons based on the percentage of common bands produced by primers, genetic similarity estimation, and diversity analysis as well as the genetic relationship among cultivars were analyzed. UPGMA obtained the dendrogram based on similarity indexes. By locating the clusters at the proper phenomic levels, the type and degree of variety between cultivars were evaluated. The software NTSYS-pc version 1.10 m was used to complete all calculations.

5. Statistical Analysis

Statistical tests were performed using SPSS Statistics 20 statistical software (IBM United Kingdom Limited, Portsmouth, UK) to determine the significance of changes obtained at different pot capacities. Where significance is indicated, a two-way ANOVA with a Tukey post-hoc test was conducted, to compare the responses of the two wheat cultivars to heat stress. Significantly different data points are labeled on figures with different letters (Dytham, 2011).

RESULTS

1. Synthesis of Iron Organic Frameworks Different Forms

1.1. Incorporation of gallic acid into iron organic frameworks

The current research concentrated on using a mixed linker technique to incorporate GA into nanoporous iron-metal organic frameworks (Fe-MOFs) (Fig. 1). First, 2-aminoterephthalic acid was used as an organic ligand, and ferrous chloride as a metal source to create Fe-MOFs. By substituting dry methanol for the guest solvent in the as-synthesized MOFs, followed by evacuation at 200°C, the activation process for Fe-MOFs were carried out (Gordon et al., 2015). Second, as in the preceding stage, mixed linker alterations enabled the effective incorporation of GA into Fe-MOFs.

1.2. Characterization

The PXRD results (Fig. 2) supported the development of Fe-MOFs. It has been demonstrated that diffraction peaks at $2\theta = 7.9^\circ, 9.4^\circ, 16.8^\circ, 18.4^\circ, 25.4^\circ,$ and 27.7° are typical of Fe-MOFs (MIL-101(Fe)-NH₂) that has been previously described (Wang and Li, 2015). Except for a modest reduction in the strength of a few peaks, all diffraction peaks in the case of GA encapsulated within Fe-MOFs were clearly recorded to be similar to Fe-MOFs. These findings support the stability of the frameworks and show that mixed linker alteration had no negative effects on Fe-MOFs.

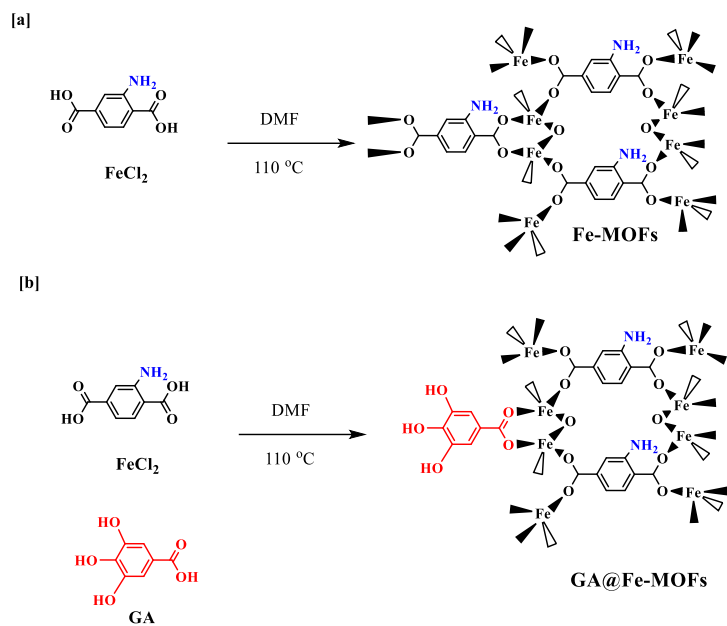


Fig. (1). A sketch represents the post synthetic modification of **a.** Fe-MOFs before GA and **b.** Fe-MOFs with GA.

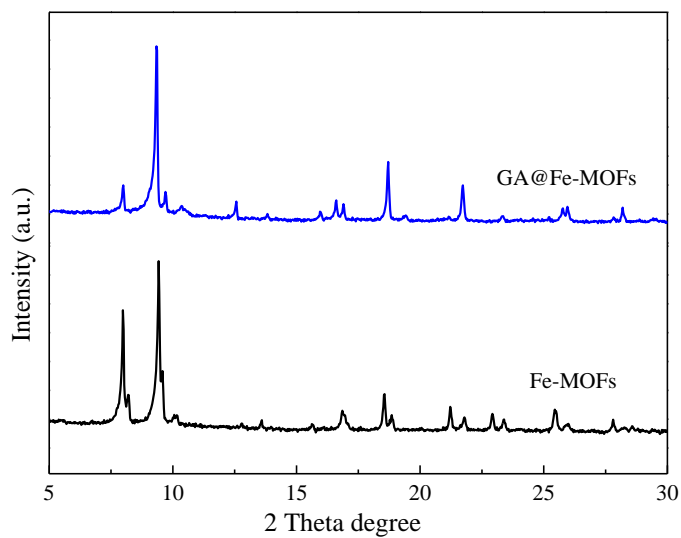


Fig. (2). X-ray diffraction patterns for Fe-MOFs, and GA encapsulated within Fe-MOFs.

Fe-MOFs were shown in the scanning electron microscopic picture to validate the creation of the purity phase. Fe-MOFs and GA encapsulated within Fe-MOFs had the same morphology with particles measuring 25*300 nm, according to a micrograph analysis (Fig. 3).

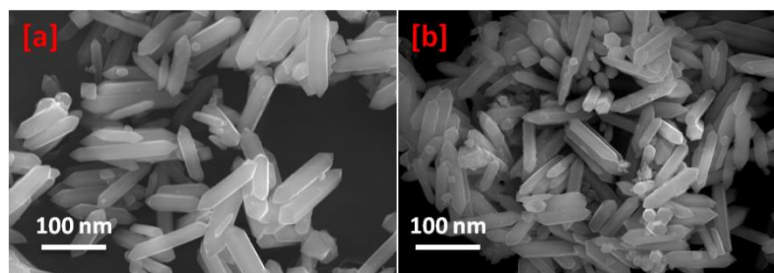


Fig. (3). Microscopic images, **a.** Fe-MOFs and **b.** GA encapsulated within Fe-MOFs.

FTIR was used to investigate GA encapsulated within Fe-MOFs and Fe-MOFs (Fig. 4). Stretching N-H vibration bands were seen in the case of Fe-MOFs at 3249 and 3329 cm^{-1} . O-C-O bond stretching and bending vibrational bands first appeared between 1600 and 1400 cm^{-1} (Vu et al., 2014). Additionally, in the range of 1500 to 1600 cm^{-1} , the aromatic ring with a C=C bond frequency was seen (Modrow et al., 2012). The Fe-O bonding of MOFs is primarily responsible for the peak measured at 545 cm^{-1} (Zhang et al., 2016). Except for a few additional bands that formed at 3418 cm^{-1} and 3018 cm^{-1} due to the -OH stretching, all characteristic bands of Fe-MOFs were seen in the case of GA encapsulated within Fe-MOFs. These new bands demonstrated that GA had been successfully incorporated.

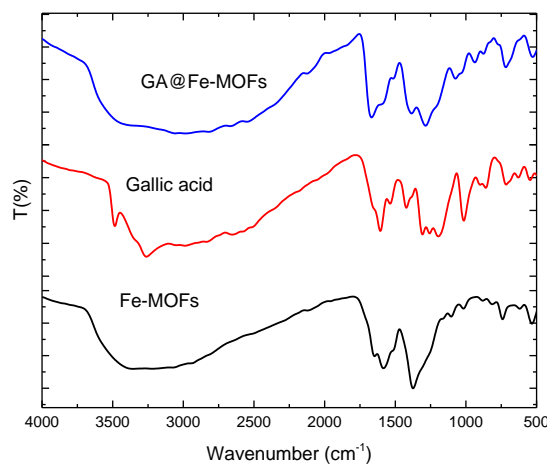


Fig. (4). FTIR spectrum for Fe-MOFs, and GA encapsulated within Fe-MOFs.

2. Yield Parameters

The results obtained in Table (3) show that approximately 24.75, 24.43, 14.06, 8.49 and 2.64% increase in wheat plant heights at harvest time after spraying with the treatments FeM4, FeM3 and FeM2, FeM1, and GA more than the control, respectively. When comparing the cultivars, the data shows that the G 171 cultivar had wheat plants that were taller at harvest than those of Gem 12 cultivar. According to the tabulated results regarding the interaction between spraying treatments and cultivars, spraying with FeM4 resulted in the cultivar G's 171 mean length reaching its maximum value. Under similar circumstances, the cultivar Gem 12 showed a higher plant height after receiving a spray treatment with FeM3. According to the findings in the same table, spraying treatments with FeM4, FeM3, FeM2, and FeM1 increased the weight of 100-seeds by 19.87, 18.54, 13.24 and 4.41% greater than heat-stressed plants, respectively. In the opposite trend, the GA spraying treatment resulted in a reduction in the weight of 100-seeds compared to the control. Regarding the cultivars, data revealed that G 171 cultivar increased the weight of 100-seeds under heat stress better than Gem 12 cultivar. According to the results, which considered the interaction between cultivars and spraying treatments, G 171 cultivar produced the highest weight of 100-seeds after spraying plants with FeM4, while Gem 12 produced the highest weight of 100-seeds when FeM3 was applied under New Valley conditions. Data in the same table also demonstrate an increase in grains and straw yield as a result of spraying treatments. When compared to heat-stressed plants, increases from spraying with FeM4, FeM3, FeM2, FeM1, and GA were, respectively, 4.76, 3.61, 2.93, 2.19 and 1.61 times greater. Spraying treatments with FeM4, FeM3, FeM2, and FeM1 in this situation similarly increased straw yield by 1.66, 1.49, 1.48 and 1.23 times higher than the control, respectively. Otherwise, there was no discernible difference between the treatment of GA spraying and the thermally stressed plants. When comparing the cultivars, data pointed out that G 171 cultivar outperformed the other cultivar in terms of improving grain output in terms of weight. On the other hand, Gem 12 exceeded G 171 in terms of straw yield under the New Valley conditions. Data collected for the interaction between the spraying treatments and cultivars demonstrate that G 171 cultivar reached its greatest mean grain yield when FeM4 was treated. When FeM4 was sprayed under heat stress conditions, Gem 12 cultivar was able to produce the largest quantity value of straw yield.

3. Biochemical Markers

3.1 Photosynthetic pigments

Data in Table (4) show that, with the exception of the GA spraying treatment, which did not significantly differ from heat-stressed plants, all spraying treatments improved the amount of pigments (a, b, and carotenoid) in wheat leaves grown under heat stress conditions. When wheat leaves were

Table (3). Effect of nanoiron-metal organic frameworks and gallic acid on yield components of two wheat cultivars under heat stress conditions.

Foliar applications	Yield components											
	Plant height (cm/plant)			100-Seeds weight (g)			Seeds weight (tons/ha)			Straw yield (tons/ha)		
	Gem 12	G 171	Mean	Gem 12	G 171	Mean	Gem 12	G 171	Mean	Gem 12	G 171	Mean
Control	85.73 f	97.47 e	91.60 E	3.79 h	5.26 c	4.53 D	0.33 h	0.48 g	0.41 F	3.61 cd	2.84 d	3.23 D
GA	88.53 f	99.50 d	94.02 D	4.28 g	4.39 f	4.33 E	0.46 g	0.85 f	0.66 E	3.48 d	2.79 e	3.13 D
FeM1	94.60 e	104.17 c	99.38 C	4.33 f	5.14 c	4.73 C	0.71 f	1.09 e	0.90 D	5.21 b	2.75 e	3.98 C
FeM2	100.52 d	108.43 bc	104.48 B	4.69 e	5.57 b	5.13 B	1.24 d	1.16 e	1.20 C	5.78 ab	3.76 cd	4.77 B
FeM3	116.80 a	111.17 b	113.98 A	4.87 d	5.88 b	5.37 A	1.48 c	1.49 c	1.48 B	5.68 b	3.96 c	4.82 B
FeM4	110.33 b	118.20 a	114.27 A	4.57 e	6.29 a	5.43 A	1.81 b	2.08 a	1.95 A	6.18 a	4.57 c	5.37 A
Mean	99.42 B	106.49 A		4.42 B	5.42 A		1.01 B	1.19 A		4.99 A	3.44 B	

Values followed by the same letter in columns are not different at $P < 0.05$ by Duncan's multiple range tests. Gem.12 : Gemmeiza 12, G 171 : Giza 171.

Table (4). Effect of nanoiron-metal organic frameworks and gallic acid on photosynthetic pigments of two wheat cultivars under heat stress conditions.

Foliar applications	Chlorophyll (a)				Chlorophyll (b)				Carotenoid			
	Gem 12	G 171	Mean		Gem 12	G 171	Mean		Gem 12	G 171	Mean	
	Photosynthetic pigments (mg g ⁻¹ FW)											
Control	0.91 e	0.92 e	0.92 E		0.58 e	0.62 d	0.60 D		0.55 e	0.57 d	0.56 BC	
GA	0.99 d	1.01 d	1.00 E		0.70 c	0.68 d	0.69 D		0.49 f	0.63 b	0.56 BC	
FeM1	1.03 d	1.17 c	1.10 D		0.77 c	0.75 c	0.76 C		0.63 b	0.67 a	0.65 A	
FeM2	1.17 c	1.34 b	1.26 C		0.86 a	0.79 b	0.83 B		0.59 c	0.54 e	0.57 B	
FeM3	1.24 b	1.78 a	1.51 A		0.89 a	0.83 b	0.86 A		0.66 a	0.59 c	0.63 A	
FeM4	1.31 b	1.56 a	1.43 B		0.81 b	0.90 a	0.85 A		0.67 a	0.49 f	0.58 B	
Mean	1.11 B	1.30 A			0.77 A	0.76 A			0.60 A	0.58 A		

Values followed by the same letter in columns are not different at $p < 0.05$ by Duncan's multiple range tests. Gem 12 : Gemmeiza 12, G 171 : Giza 171.

sprayed with FeM4, FeM3, FeM2 and FeM1 treatments, respectively, the tabulated data show an improvement in chlorophyll a by 1.55, 1.64, 1.37 and 1.2 times and an increase in chlorophyll b by 1.42, 1.43, 1.38 and 1.27 times more than the control for each, respectively. The cultivar G 171 had the highest level of chlorophyll a in contrast to Gem 12 cultivar when the two cultivars were compared. However, data revealed no discernible changes in chlorophyll b levels between the two cultivars under New Valley conditions. In terms of the interaction between foliar treatments and cultivars, results showed that G 171 cultivar had the highest level of chlorophyll a when FeM3 was used. The research also showed that when FeM4 and FeM3 were applied to wheat leaves, respectively, G 171 and Gem 12 cultivars produced the highest levels of chlorophyll b. Data showed that providing spray treatments with FeM1 and FeM3 significantly increased the carotenoid content of wheat leaves. The findings revealed no discernible differences between the two wheat cultivars when comparing them. The research indicated that G 171 and Gem 12 cultivars produced the highest levels of carotenoid when sprayed with FeM1 and FeM4, respectively. This impact was related to the interaction between the spray treatments and cultivars.

3.2. Free proline

According to the data in Table (5), following spraying with nanoscale treatments, the concentration of compatible salutes like free proline and glycinebetaine in wheat leaves grown under heat stress sharply decreased. When using the spray with treatments FeM4, FeM3, FeM2, FeM1, and GA data show that the free proline content of wheat leaves was reduced by 59.73, 55.13, 41.35, 36.22 and 21.62% less than that of heat-stressed plants, respectively. The findings revealed no discernible differences between the two wheat cultivars when comparing them. The cultivar G 171 outperforms Gem 12 cultivar in lowering free proline concentration in wheat leaves when the spray was treated with FeM4 according to the study on the relationship between spray treatments and cultivars.

3.3. Glycinebetaine

In Table (5), when FeM4, FeM3, FeM2, FeM1, and GA were sprayed on wheat leaves, they reduced the amount of glycinebetaine by 23.99, 21.58, 17.86, 14.23 and 11.28% less than that of heat-stressed plants, respectively. In comparison to the other cultivar, the results indicated that Gem 12 was more effective at lowering the level of glycinebetaine. The highest mean decrease of glycinebetaine was achieved by Gem 12 cultivar when it was sprayed with FeM4, according to the investigation of the interaction between wheat cultivars and spraying treatments.

3.4. Peroxidase

According to the findings presented in the Table (5), spraying with FeM4, FeM3, FeM2, FeM1, and GA, respectively, increased the peroxidase enzyme activity in wheat leaves by 1.40, 1.48, 1.32, 1.30, and 1.13 times more

Table (5). Effect of nanoiron-metal organic frameworks and gallic acid on proline, glycinebetaine and peroxidase of two wheat cultivars under heat stress conditions.

Foliar applications	Proline ($\mu\text{moles proline g}^{-1}\text{FW}$)			Glycinebetaine ($\mu\text{moles GB g}^{-1}\text{DW}$)			POD ($\Delta\text{Abs/mg S. protein/3 min}$)		
	Gem 12	G 171	Mean	Gem 12	G 171	Mean	Gem 12	G 171	Mean
Control	3.68 a	3.71 a	3.70 A	197.02 b	238.62 a	217.82 A	1.22 f	1.19 f	1.21 D
GA	2.88 b	2.92 b	2.90 B	187.42 c	199.06 b	193.24 B	1.35 e	1.40 d	1.37 C
FeM1	2.48 b	2.24 c	2.36 C	178.33 d	195.33 b	186.83 C	1.48 c	1.66 bc	1.57 B
FeM2	2.25 c	2.09 cd	2.17 C	170.22 de	187.60 c	178.91 D	1.69 b	1.52 c	1.60 B
FeM3	1.86 d	1.46 e	1.66 D	162.05 e	179.57 d	170.81 D	1.73 b	1.86 a	1.79 A
FeM4	1.63 d	1.35 e	1.49 E	158.10 e	173.02 de	165.56 E	1.42 d	1.97 a	1.69 A
Mean	2.46 A	2.29 A		175.52 B	195.53 A		1.48 B	1.60 A	

Values followed by the same letter in columns are not different at $p < 0.05$ by Duncan's multiple range tests. FW: Fresh weight, DW: Dry weight, GB: Glycinebetaine, Gem 12: Gemmeiza 12, G 171: Giza 171.

than the control. In terms of wheat cultivars, G 171 cultivar outperformed Gem 12 cultivar in terms of peroxidase activity on average. The cultivar G 171 had the highest degree of peroxidase enzyme activity when its leaves were sprayed with FeM4, according to the results, which considered the interaction between spraying treatments and wheat cultivars.

3.5. Superoxide dismutase isozymes

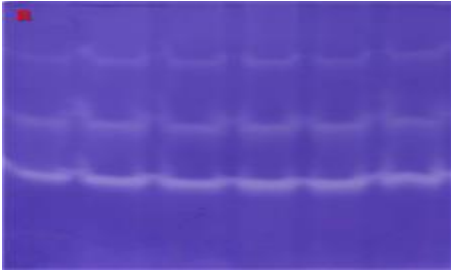
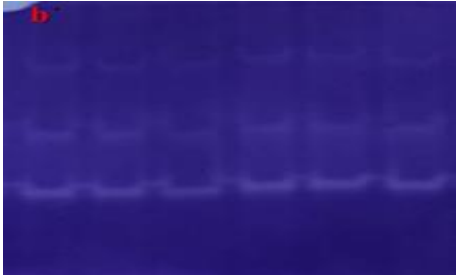
For the two wheat cultivars shown in Table (6), in the current experiment, SOD patterns showed that there were around three bands present. With all foliar application treatments, the more intensive band was displayed at band number 3 in the two wheat cultivars. Data on the band intensity of Gem 12 cultivar showed that treatments, with the exception of foliar applications with FeM2 and FeM3 for band number 2, decreased bands number 2 and 3 compared to the control. In the opposite direction, all treatments, except for the foliar application of FeM1, resulted in an increased in band number 1. Band number 1 of G 171 cultivar's band intensity decreased in comparison to the control after plants were sprayed with all foliar treatments. Other than treatments with FeM2 for band number 2 and treatments with GA for band number 3, bands number 2 and 3 were increased after treatments with all foliar sprays.

3.6. Proteins electrophoretic patterns

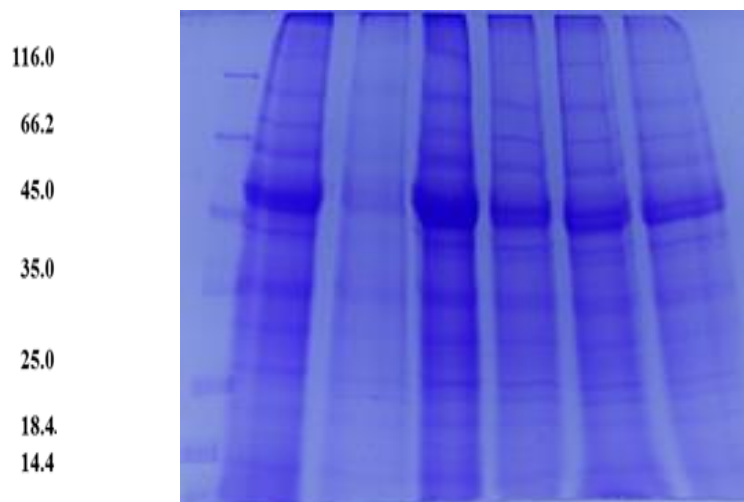
Tables (7 and 8) exhibit and depict the results of SDS-polyacrylamide electrophoresis of soluble protein recovered from leaves of the two wheat cultivars (Gem 12 and G 171) sprayed with GA, FeM1, FeM2, FeM3, and FeM4 under heat stress conditions. The samples from Gem 12 were resolved into 10 to 12 bands with molecular weights ranging from 18.7 to 160.7 kDa, according to gel analysis. Additionally, G 171 samples were separated into 9 to 11 bands with molecular masses ranging from 18.7 to 160.7 kDa. For Gem 12 cultivar, the band with a molecular weight of 160.7 kDa vanished when all spraying treatments were added, with the exception of the GA spraying treatment, in comparison to the control. At the same time, the same band appeared for G 171 cultivar when GA and FeM1 were sprayed on the plants, in contrast to the untreated ones. Except for spraying with FeM2 and FeM3 compared to the control for G 171 cultivar, the band with a partial weight of 141.7 kDa vanished from all spraying treatments. Additionally, the appearance of the band with a molecular weight of 112.2 kDa following GA, FeM1, and FeM2 spray treatments was compared to G 171 cultivar's control. Additionally, data was noted that the band of the two wheat cultivars with a partial weight of 91.5 kDa vanished following GA spray treatment, and it also vanished after spraying plants from G 171 cultivar with FeM1 and FeM2. For the cultivar Gem 12 the band with a molecular weight of 74.8 kDa vanished following all spraying treatments except for the GA treatment, whereas the same band appeared following all spraying treatments except for the spraying treatment with FeM3 in comparison to the control for G 171 cultivar. In contrast to the control of Gem 12 cultivar, the band with a molecular weight

of 55.5 kDa appeared in plant samples after the addition of all spraying treatments aside from the spraying with GA. For Gem 12 cultivar, the band with a molecular weight of 24.6 vanished after treatment with GA spray. In contrast to the control of G 171 cultivar, the band with a molecular weight of 20.5 appeared in plant samples after spraying the treatments with FeM2, FeM3, and FeM4.

Table (6). Effect of nanoiron-metal organic frameworks and gallic acid on SOD isozymes in two wheat cultivars under heat stress conditions.

Gemmeiza 12						
						
Band numbers	Band intensity					
	Control	GA	FeM1	FeM2	FeM3	FeM4
1	1.02	1.39	1.00	1.27	1.44	1.17
2	1.93	1.84	1.68	2.00	1.97	1.74
3	2.62	2.43	2.25	2.51	2.46	2.44
Total bands	3	3	3	3	3	3
Giza 171						
						
Band numbers	Band intensity					
	Control	GA	FeM1	FeM2	FeM3	FeM4
1	1.60	1.40	1.50	1.00	1.60	1.24
2	1.97	1.92	2.21	1.24	2.45	2.29
3	2.78	2.68	3.39	2.79	3.07	2.81
Total bands	3	3	3	3	3	3

Where; 1.00: refers to lowest band intensity, 3.39: refers to highest band intensity for Giza 171 and 2.62: refers to highest band intensity for Gemmeiza 12.

Table (7). Effect of nanoiron-metal organic frameworks and gallic acid on soluble protein profile of wheat (Gemmeiza 12) under heat stress conditions.

Band numbers	Molecular weight (kDa)	Band intensity					
		Control	GA	FeM1	FeM2	FeM3	FeM4
1	160.7	1.27	1.20	0.00	0.00	0.00	0.00
2	141.7	0.00	0.00	0.00	0.00	0.00	0.00
3	112.2	1.21	1.33	2.34	2.21	1.67	1.52
4	91.5	1.94	0.00	2.37	2.58	2.46	2.01
5	74.8	1.49	1.13	0.00	0.00	0.00	0.00
6	62.2	2.36	2.11	2.20	2.40	1.77	2.06
7	55.5	0.00	0.00	3.47	3.04	2.66	2.42
8	43.7	5.24	4.57	8.48	6.06	5.28	5.38
9	35.7	2.19	1.90	1.50	2.02	2.77	2.25
10	28.2	3.32	3.10	4.38	3.67	3.00	2.90
11	24.6	1.59	0	2.87	1.65	2.38	1.83
12	21.6	1.99	1.74	1.91	2.30	2.25	1.93
13	20.5	2.02	1.42	2.48	1.86	1.44	1.00
14	18.7	2.67	1.20	2.23	1.78	1.87	1.59
Total bands		12	10	11	11	11	11

Where; 0: the absence of band, 1.00: refers to lowest band intensity, 8.48: refers to highest band intensity.

Table (8). Effect of nanoiron-metal organic frameworks and gallic acid on soluble protein profile of wheat (Giza 171) under heat stress conditions.

Band numbers	Molecular weight (kDa)	Band intensity					
		Control	GA	FeM1	FeM2	FeM3	FeM4
1	160.7	0.00	1.45	1.13	0.00	0.00	0.00
2	141.7	1.33	0.00	0.00	1.32	1.35	0.00
3	112.2	0.00	1.70	2.20	1.47	0.00	0.00
4	91.5	2.06	0.00	0.00	0.00	1.89	2.04
5	74.8	0.00	1.91	1.00	1.96	0.00	1.81
6	62.2	1.76	2.00	2.38	1.15	1.58	1.87
7	55.5	0.00	0.00	0.00	0.00	0.00	0.00
8	43.7	2.84	5.11	3.22	4.28	3.81	3.71
9	35.7	1.82	2.69	2.43	1.61	1.78	1.91
10	28.2	2.56	3.49	3.69	2.37	2.58	2.76
11	24.6	1.22	2.84	2.35	2.01	1.72	2.75
12	21.6	1.01	2.04	1.65	2.13	2.14	1.95
13	20.5	0.00	0.00	0.00	1.38	1.35	1.43
14	18.7	1.91	2.67	2.57	1.84	2.32	2.76
Total bands		9	10	10	11	10	10

Where; 0: the absence of band, 1.00: refers to lowest band intensity, 5.11: refers to highest band intensity.

4. Molecular Marker

4.1. Inter-simple sequence repeats (ISSR-PCR technique)

The information shown in Table (9) and Fig. (5) demonstrates the use of six primers by the ISSR technique on wheat samples to identify similarities and differences between Gem 12 and G 171 wheat cultivars following the application of FeM1 and FeM4 compared to untreated plants for each, during heat stress. With a band size range of 150 to 550 bp, the initial primer, ISSR-1, produced 12 bands, of which 9 were monomorphic and 3 were polymorphic. Two positive specific bands measuring 160 and 180 bp and one negative specific polymorphic band measuring 150 bp made up the three polymorphic bands. With the polymorphism frequency was 86% and the polymorphic percentage was 25%, in Gem 12 cultivar. The identical ISSR-1 primer produced eleven bands with sizes ranging from 160 to 550 bp, including two negative specific bands with diameters of 160 and 340 bp and nine monomorphic bands. Also, the polymorphism frequency was 94% and the polymorphism percentage was 18%, for G 171 cultivar. Additionally, it was discovered that a band with a size of 150 bp separated the cultivar Gem 12 from the cultivar G 171.

Eight bands in the two wheat cultivars with widths ranging from 160 to 700 bp were produced by primer No. 2, ISSR-2. The eight bands had the percentage of polymorphism of 12.5% with a frequency of 91% for Gem 12 and were composed of seven monomorphic bands and one polymorphic band as a positive specific band with a band size of 230 bp. In contrast to G 171 cultivar, this primer did not demonstrate any differences.

Table (9). Effect of foliar applications with FeM1 and FeM4 on polymorphism of two wheat cultivars under heat stress conditions.

Primers name	Band size (bp)	Total number of bands	Monomorphic bands	Polymorphic bands	Polymorphic percentage bands (%)	Frequency
Gemmeiza 12						
ISSR-1	150-550	12	9	3	25	0.86
ISSR-2	160-700	8	7	1	12.5	0.91
ISSR-3	200-700	11	11	0	0	1.0
ISSR-4	250-1150	14	8	6	42.86	0.74
ISSR-5	220-1400	11	11	0	0	1.0
ISSR-6	280-1150	11	8	3	27	0.85
Giza 171						
ISSR-1	160-550	11	9	2	18	0.94
ISSR-2	160-700	8	8	0	0	1.0
ISSR-3	200-700	10	9	1	10	0.93
ISSR-4	250-1050	13	8	5	38.46	0.79
ISSR-5	220-1400	11	11	0	0	1.0
ISSR-6	240-1150	12	9	3	25	0.89

FeM1: Fe-MOFs and FeM4: 40% GA encapsulated within Fe-MOFs

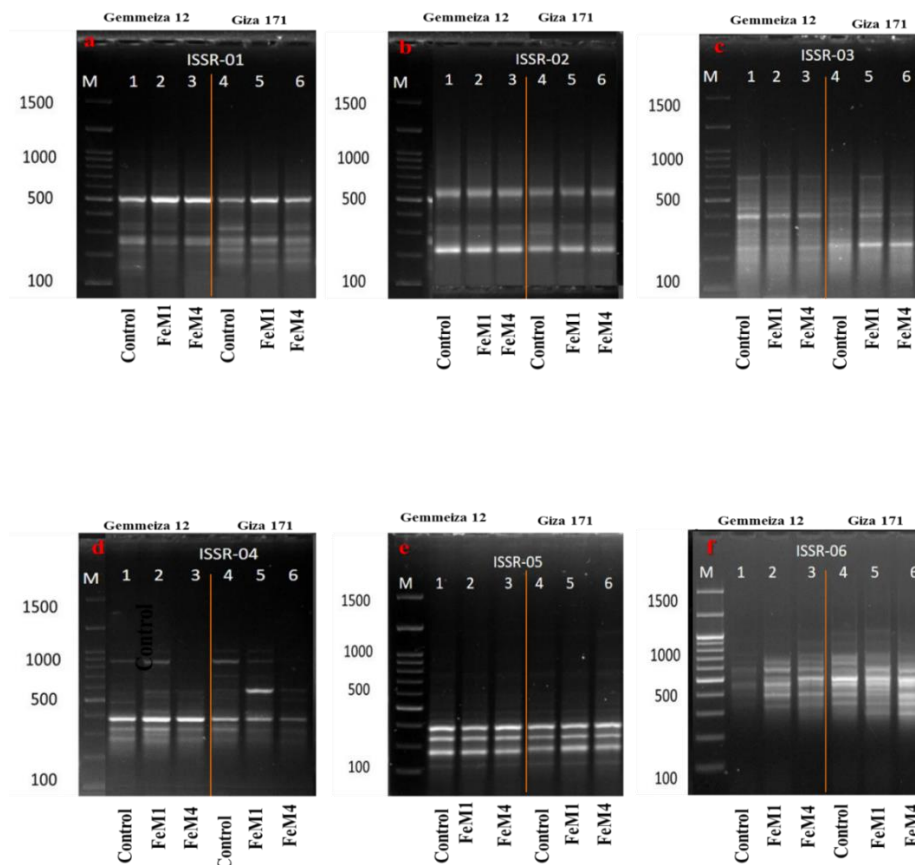


Fig. (5). Effect of foliar applications of Fe-MOFs and 40% GA encapsulated within Fe-MOFs on the polymorphism of two wheat cultivars Gemmeiza 12 and Giza 171 under heat stress conditions.

Gem 12 cultivar and ISSR-3 yielded identical eleven bands with sizes ranging from 200 to 700 bp. Compared to G 171 cultivar, the results revealed the existence of ten bands, with sizes ranging from 200 to 700 bp, including nine monomorphic bands and one polymorphic band as a positive specific band with a band size of 520 bp. With a frequency of 93%, polymorphism was 10% in proportion. Additionally, ISSR-3 was employed to measure a band with a 280 bp width and was found to be present in cultivar Gem 12 while lacking in cultivar G 171.

The findings in the same table and figure demonstrate that ISSR-4 produced fourteen bands, ranging in size from 250 to 1150 bp, of which eight are monomorphic bands and six polymorphic bands, with four negative specific bands at band sizes 400, 680, 1050, and 1150 bp and two positive

specific bands at band sizes 280 and 490 bp. The percentage of polymorphism was 42.86%, with a frequency of 74% for Gem 12 cultivar. In the same direction, ISSR-4 broadcasts 13 bands with sizes ranging from 250 to 1050 bp, including eight monomorphic bands and five polymorphic bands defined as follows: two negative bands defined with sizes 680 and 1050 bp, and three positive bands defined with sizes 400 and 450 bp. The amount of polymorphism was 38.46%, with a frequency of 79% for G 171 cultivar. The presence of two bands with sizes of 280 and 1150 bp allowed the cultivar Gem 12 to be identified from the cultivar G 171. While G 171 cultivar was separated from Gem 12 cultivar by having a band size of 540 bp, these distinctions only became apparent when ISSR-4 technology was used to analyze the samples.

The ISSR-5 primer produced 11 monomeric bands with widths ranging from 220 to 1400 bp, as shown by the results in the same table and figure. This primer did not exhibit any changes in response to treatment between the two wheat cultivars.

The ISSR-6 offered 11 bands, eight of which were monomorphic and three of which were polymorphic, ranging in size from 280 bp to 1150 bp, one negative specific band at 660 bp and two positive specific bands at 430 bp and 1150 bp in size. For Gem 12, the polymorphism frequency was 85% and the polymorphic rate was 27%. Furthermore, ISSR-6 offered 12 bands, nine of which were monomorphic and three of which were polymorphic, ranging in size from 240 to 1150 bp, one positively defined band of size 430 bp and two negatively defined bands of size 240 bp and 1150 bp. For the cultivar G 171, the polymorphism frequency was 89%, with the polymorphic rate of 25%.

When compared to other primers, it was shown that ISSR-4, ISSR-6, and ISSR-1 were the most specialized primers that can distinguish between different wheat cultivars and spray treatments. When employed with Gem 12 cultivar, however, ISSR-5 and ISSR-3 were ineffective and did not exhibit any differences. Additionally, ISSR-5 and ISSR-2 revealed no variations from G 171 cultivar.

5. Similarity Matrix

Data in Table (10) display the percentage similarity between Gem 12 and G 171 wheat cultivars following the addition of FeM1 and FeM4 spray treatments in comparison to the control for each. According to the data in the table, the treatment of FeM1 for Gem12 cultivar and the treatment of FeM4 for G 171 cultivar had the lowest similarity percentage of 87%. The G 171 cultivar's FeM1 and FeM4 had a 96% similarity rate, which was the greatest possible.

6. Phylogenetic Tree

ISSR approach was used to create a tree graph (Fig. 6) that illustrates the evolutionary link between the wheat samples under investigation and the spraying treatments. Following a two-cluster division, samples 1, 2, and 3 of

Gem 12 cultivar were included in the first cluster. The genetic tree was also able to place sample number 1, the control, in a different sub-cluster from samples 2 and 3, which represented spray treatments with FeM1 and FeM4 for the same cultivar, respectively. Likewise, samples 4, 5, and 6 of G 171 cultivar variation were part of the second cluster. Using ISSR method, the genetic tree was also able to group sample number 4 as a control into a single sub-cluster while classifying sample number 5, which represented the treatment of FeM1, and 6, which represented the treatment of FeM4, into separate sub-clusters.

Table (10). Effect of foliar applications with FeM1 and FeM4 on similarity matrix and cluster analysis of two wheat cultivars under heat stress conditions.

Wheat cultivar	Foliar applications	Gem 12			G 171		
		Control	FeM1	FeM4	Control	FeM1	FeM4
Gem 12	Control	1.00					
	FeM1	0.93	1.00				
	FeM4	0.93	0.94	1.00			
G 171	Control	0.92	0.91	0.89	1.00		
	FeM1	0.92	0.91	0.89	0.94	1.00	
	FeM4	0.90	0.87	0.88	0.94	0.96	1.00

Gem 12: Gemmeiza 12, G 171: Giza 171, FeM1: Fe-MOFs and FeM4: 40% GA encapsulated within Fe-MOFs.

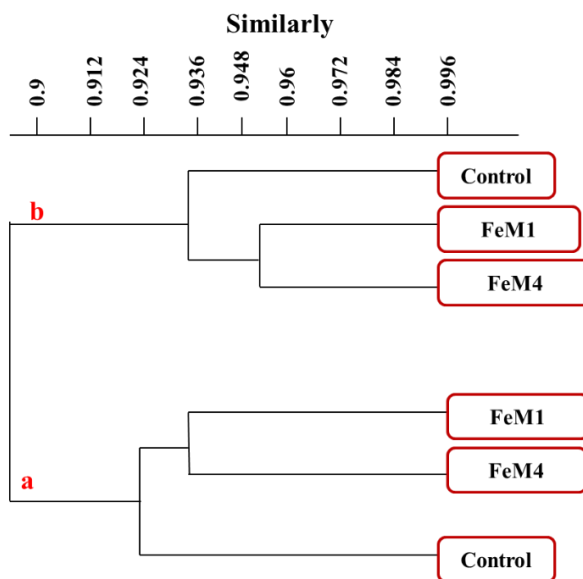


Fig. (6). Dendrogram and similarity matrix of two wheat cultivars **a.** Gemmeiza 12 and **b.** Giza 171 as affected by foliar applications of Fe-MOFs and 40%GA encapsulated within Fe-MOFs.

DISCUSSION

1. Yield Parameters

The evidence that is now available suggests that nano-composite considerably enhance plant growth and development while reducing the detrimental effects of heat stress on wheat plants. The outcomes obtained are supported by Ahmed et al. (2021) and Mahmoud and Abdelhameed (2022). The increase in yield production might be connected to 1) Through the leaves, nano-composite penetrate the plant and cause biochemical, morphological, molecular, and physiological changes that may have a big effect on the plant's growth as boosts lateral root formation, root biomass, root hydraulic conductivity, gene expression, and hormonal signals, enabling improved water uptake and the transport of different solutes across the membrane and ensuring improved plant growth under environmental stress (Das and Das, 2019 and Ahmed et al., 2022) and ability to produce crops (Khan et al., 2019 and Mahmoud and Abdelhameed, 2021). 2) Nutrient uptake, Nitrate reductase activity, and N absorption are all greatly improved by foliar spraying of nanoparticles, which also increase crop yield and improve protein and amino acid synthesis (Yuan et al., 2013 and Mahmoud et al., 2022b). Nanoparticles improve osmolality, nutrients, and amino acids, which increases antioxidant activities and protects wheat plants from oxidative stress, and boosts seed and straw yield. Also increase the activity of antioxidant enzymes and enhance non-enzymatic antioxidants like phenolic compounds (El-Zohri et al., 2021 and Ahmed et al., 2022). Furthermore, the exogenous spray of nanoparticles administration preserved cell hydration status and membrane stability during abiotic stress, increasing the water uptake, effectiveness of PS-II, and metabolic activities. Consequently, there was an increase in yield production (Semida et al., 2021 and Ahmed et al., 2022).

2. Photosynthetic Pigments

Heat stress lowers the rate of electron flow, PS-II efficiency, and chlorophyll synthesis, all of which have a negative effect on the overall effectiveness of plant photosynthesis. The nano-composite (GA encapsulated within Fe-MOFs) mitigated the negative effect of high temperature on photosynthetic pigments, as shown by the results above, and these findings were highly corroborated by Mahmoud and Abdelhameed (2022 and 2023). The development of photosynthetic pigments could be connected to nano-composite can lessen the harmful effects of heat stress by lowering the buildup of hydrogen peroxide and malondialdehyde this maintained a greater absorption of carbon dioxide and helped control stomatal conductivity while maintaining the effectiveness of the photosynthetic mechanism (Mahmoud and Abdelhameed, 2022). Additionally, nanoparticles can enter plant chloroplasts and reach the PS-II reaction center, increasing electron transmission, light absorption in the chloroplasts, chlorophyllase activity, and enhancing photosynthesis efficiency and plant development (Maity et al.,

2018). Additionally, nanoparticles enhance gene expression (LHCII-b) in the thylakoid membrane, which encourages light absorption in chloroplasts (Ze et al., 2011). Moreover, nanoparticles enhance RuBisCO activity, nitrogen absorption, and nitrate reductase activity, all of which lead to improved photosynthetic performance and efficiency in plants under abiotic stress (Yuan et al., 2013 and Mahmoud et al., 2022b). Also, antioxidant enzymes that guard against oxidation of chlorophyll become more active while under stress (Mahmoud et al., 2022b).

3. Free Proline and Glycinebetaine

When a plant is under stress, its immune system normalizes the buildup of osmoles such as free proline and glycinebetaine, which strengthens the antioxidant systems and lessens oxidative damage (Shabala and Cui, 2006 and Dar et al., 2016). Previous research indicated that free proline and glycinebetaine levels in wheat shoots reduced because of nano-composite treatments on the accumulation of suitable solutes. These outcomes were completely consistent with Carillo et al. (2011) and Hendawey and Kamel (2015). The lowering compatible solute levels after nano-composite treated may be related, indeed, the activity of antioxidant enzymes can be increased by nanoparticles, and this minimizes the buildup of reactive oxygen species in plants, alleviating stress on the plants (Usman et al., 2020). Furthermore, glycinebetaine interacts with molecules and structures, maintains macromolecule activity, and protects membrane integrity from stressors by scavenging ROS. It also plays a significant role in osmoregulation. With restrictions on the buildup of reactive oxygen species and lipid peroxidation, it can promote the expression of genes involved in oxidative stress responses and even stabilize chlorophyll structures under stress (Annunziata et al., 2019). A reverse reaction for the synthesis of proline and glycinebetaine would result from this. Additionally, proline production is inhibited by hydroxyproline, which nanoparticles stimulate in order to decrease glycinebetaine buildup (Carillo et al., 2008). In addition, proline and glycinebetaine are transferred from fully developed tissues to tiny, developing tissues for the synthesis of proteins and amino acids, the latter of which are more sensitive to stress. Strong light entirely inhibits the glycinebetaine synthesis in wheat (Carillo et al., 2011).

4. Antioxidant Enzymes (POD and SOD)

GA, a phenolic molecule, and nanoparticles (Fe-MOFs) work well together as an antioxidant combination to reduce the harmful effects of heat stress on wheat plants. According to the information in Tables (5 and 6), spraying the treatments with nano-composite led to an increase in the activity of the antioxidant enzymes peroxidase and superoxide dismutase. The results obtained are consistent with the earlier ones (Sutulienė et al., 2021 and Mahmoud and Abdelhameed, 2022). The rise in antioxidant enzyme activity could be caused by antioxidant gene expression is enhanced by nanoparticles

(Mittal et al., 2020). Likewise, it induces oxidative stress in plants under abiotic stress conditions by raising the buildup of MDA, H₂O₂, and ROS that cause oxidative stress. This stimulation of plant immune system activity then boosts the activity of antioxidant enzymes (Hendawey et al., 2018). In the same environment, under abiotic stress that increased SOD activity, nanoparticles also enhance the relative abundance of the Cu/Zn-SOD band (Rasheed et al., 2022). Additionally much more nanoparticles promote the buildup of carbohydrates, which boosts the activity of antioxidant enzymes (Heikal et al., 2022).

5. Proteins Electrophoretic Patterns

The information in Tables (7 and 8) provides an overview of the soluble protein findings for several samples of G 171 and Gem 12 wheat cultivars. Results from earlier tests are supported by Nazir et al. (2021) and Mahmoud and Abdelhameed (2022). The increased protein bands density and the rise in protein bands in wheat plants treated with nano-composite GA encapsulated within Fe-MOFs' potential participation in the induction of proteins and enzymes involved in the electron transport chain, glycolysis, protein synthesis, and redox homeostasis in promoting heat stress tolerance was discovered by proteomic investigations on heat stress in wheat (Narayanan et al., 2015 and Wang et al., 2015). Other factors that contribute to heat stress tolerance include higher levels of heat shock proteins, inhibit or activate anabolism, sucrose synthesis, glutathione S-transferase, and antioxidant enzymes. RuBisCO activase A and PEP carboxylase, two essential proteins involve in photosynthesis and signal transduction, glycolysis, stress defense, heat shock and ATP production may be up-regulated as a result of the nano-composite (Wang et al., 2015). The plant cell starts to synthesize in response to heat stress, heat shock proteins (HSPs) are a class of unique proteins (Waters et al., 1996). Moreover, the primary defense against heat stress entails the buildup of several osmolytes, including proline, glycinebetaine and antioxidant enzymes (Apse and Blumwald, 2002 and Riazud-Din et al., 2010). Wheat accumulates proline when exposed to heat stress (Hamada and El-Enany, 1994).

6. ISSR-PCR Technique

ISSR shows the effect of spraying treatments with nanometer compounds on the two wheat cultivars (G 171 and Gem 12) cultivated in high temperatures by referring to Fig. (5). It is evident from the molecular investigation that G 171 is more genetically stable than Gem 12, the percentage of polymorphism varied between 10% (ISSR-3) and 38.46% (ISSR-4), with an average of 24.23% for G 171 cultivar. As well as, in Gem 12 cultivar the percentage of polymorphism varied between 12.5% (ISSR-2) and 42.86% (ISSR-4), with an average of 27.68% (Table 9) cultivar observed decreased polymorphism (Fig. 5). The tree plot showed that ISSR markers successfully separated the tested cultivars into two distinct groups according

to cultivar type and spray treatments (Fig. 6). The collected data were entirely consistent with the research by Bordes et al. (2014) and Kidane et al. (2017). They looked at genetic loci in wheat that are linked to changes in grain production, disease resistance, milling quality, kernel size, and other agronomic variables. The alterations in the ISSR profile showed that the dose and kind of the nanoparticles used caused genetic variance. The ISSR profile can be utilized to identify mutations, which are most likely the result of DNA damage or rearrangements brought on by nanoparticles-induced genetic variation (Mahdi et al., 2021).

CONCLUSION

Wheat crop productivity is significantly affected by high temperatures. The study focused on the use of GA, a phenolic chemical and growth promoter, and Fe-MOFs, a nano-composite that boosts plant tolerance to environmental stresses and a growth promoter, to encourage wheat plants to tolerate heat stress and lessen the damage caused by it. According to the study, the activity of the peroxidase and superoxide dismutase enzymes increased, and there was no discernible difference in grain yield when GA compound alone was sprayed on wheat seedlings. Additionally, the yield of wheat was only marginally increased by Fe-MOF spraying alone. Wheat plants were more tolerant to heat stress when GA was loaded on Fe-MOFs in the percentages of 20, 30 and 40%. This tolerance was visible in plant growth and development. Wheat seedlings under heat stress were sprayed with FeM4, which increased the output of proteins, particularly heat shock proteins. This was achieved by increasing the quantity and density of the protein bands, which in turn increased the size of the wheat grains and the weight of the 100-seeds, improving the wheat yield. Because there were no alterations at the genome level and consequently no mutations harming the health of wheat consumers because of plants sprayed with GA encapsulated within Fe-MOFs, the genetic analysis further demonstrated the safety of these substances. Compared to Gem 12 cultivar, whose genetic stability was 87%, G 171 cultivar maintained genetic stability of 96% better.

REFERENCES

- Abdelhameed, R.M., R.E. Abdelhameed and H.A. Kamel (2019). Iron-based metal-organic-frameworks as fertilizers for hydroponically grown *Phaseolus vulgaris*. *Materials Letters*, 237: 72-79.
- Ahmed, J. and M. Hassan (2011). Evaluation of seedling proline content of wheat genotypes in relation to heat tolerance. *Bangladesh Journal of Botany*, 40 (1): 17-22.
- Ahmed, T., M. Noman, N. Manzoor, M. Shahid, M. Abdullah, L. Ali, G. Wang, A. Hashem, A.B.F. Al-Arjani and A.A. Alqarawi (2021). Nanoparticle-based amelioration of drought stress and cadmium

- toxicity in rice via triggering the stress responsive genetic mechanisms and nutrient acquisition. *Ecotoxicology and Environmental Safety*, 209: 111829.
- Ahmed, H.B., N.E. Mahmoud, A.A. Mahdi, H.E. Emam and R.M. Abdelhameed (2022). Affinity of carbon quantum dots anchored within metal organic framework matrix as enhancer of plant nourishment. *Heliyon*, 8 (12): 1-13.
- Alabdallah, N.M., M.M. Hasan, I. Hammami, A.I. Alghamdi, D. Alshehri and H.A. Alatawi (2021). Green synthesized metal oxide nanoparticles mediate growth regulation and physiology of crop plants under drought stress. *Plants*, 10 (8):1730.
- Allison, L. and L.A. Richards (1954). In: 'Diagnosis and Improvement of Saline and Alkali Soils'. Vol 60. Soil and Water Conservative Research Branch, Agricultural Research Service, USA.
- Almeselmani, M., P. Deshmukh, R.K. Sairam, S. Kushwaha and T. Singh (2006). Protective role of antioxidant enzymes under high temperature stress. *Plant Science*, 171 (3): 382-388.
- Anderson, J.A., G. Churchill, J. Autrique, S. Tanksley and M. Sorrells (1993). Optimizing parental selection for genetic linkage maps. *Genome*, 36 (1): 181-186.
- Annunziata, M.G., L.F. Ciarmiello, P. Woodrow, E. Dell'Aversana and P. Carillo (2019). Spatial and temporal profile of glycine betaine accumulation in plants under abiotic stresses. *Frontiers in Plant Science*, 10: 230.
- Apse, M.P. and E. Blumwald (2002). Engineering salt tolerance in plants. *Current Opinion in Biotechnology*, 13 (2): 146-150.
- Asseng, S., F. Ewert, P. Martre, R.P. Rötter, D.B. Lobell, D. Cammarano, B.A. Kimball, M.J. Ottman, G.W. Wall and J.W. White (2015). Rising temperatures reduce global wheat production. *Nature Climate Change*, 5 (2): 143-147.
- Bates, L.S., R. Waldren and I. Teare (1973). Rapid determination of free proline for water-stress studies. *Plant and Soil*, 39: 205-207.
- Bindra, P., K. Kaur, A. Rawat, A. De Sarkar, M. Singh and V. Shanmugam (2019). Nano-hives for plant stimuli controlled targeted iron fertilizer application. *Chemical Engineering Journal*, 375: 121995.
- Bordes, J., E. Goudemand, L. Duchalais, L. Chevarin, F.X. Oury, E. Heumez, A. Lapiere, M.R. Perretant, B. Rolland and D. Beghin (2014). Genome-wide association mapping of three important traits using bread wheat elite breeding populations. *Molecular Breeding*, 33 (4): 755-768.
- Braun, H.-J., G. Atlin and T. Payne (2010). Multi-Location Testing as a Tool to Identify Plant Response to Global Climate Change. In: 'Climate Change and Crop Production'. CABI Wallingford UK, pp. 115-138.

- Carillo, P., G. Mastrolonardo, F. Nacca, D. Parisi, A. Verlotta and A. Fuggi (2008). Nitrogen metabolism in durum wheat under salinity: accumulation of proline and glycine betaine. *Functional Plant Biology*, 35 (5): 412-426.
- Carillo, P., D. Parisi, P. Woodrow, G. Pontecorvo, G. Massaro, M.G. Annunziata, A. Fuggi and R. Sulpice (2011). Salt-induced accumulation of glycine betaine is inhibited by high light in durum wheat. *Functional Plant Biology*, 38 (2): 139-150.
- Challinor, A.J., J. Watson, D.B. Lobell, S. Howden, D. Smith and N. Chhetri (2014). A meta-analysis of crop yield under climate change and adaptation. *Nature Climate Change*, 4 (4): 287-291.
- Chutipaijit, S., S. Cha-Um and K. Sompornpailin (2009). Differential accumulations of proline and flavonoids in indica rice varieties against salinity. *Pakistan Journal of Botany*, 41 (5): 2497-2506.
- Dar, M.I., M.I. Naikoo, F. Rehman, F. Naushin and F.A. Khan (2016). Proline accumulation in plants: roles in stress tolerance and plant development. In: 'Osmolytes and plants acclimation to changing environment: emerging omics technologies', pp. 155-166. DOI: 10.1007/978-81-322-2616-1_9.
- Das, A. and B. Das (2019). Nanotechnology a potential tool to mitigate abiotic stress in crop plants. In: 'Abiotic and Biotic Stress in Plants'. IntechOpen, pp. 1-13. DOI:10.5772/intechopen.83562.
- Doyle, J.J. and J.L. Doyle (1987). A rapid DNA isolation procedure for small quantities of fresh leaf tissue. *Phytochemical Bulletin*, 19: 11-15.
- Dytham, C. (2011). In: 'Choosing and Using Statistics: A biologist's Guide'. John Wiley and Sons Ltd., UK.
- El-Zohri, M., N.A. Al-Wadaani and S.O. Bafeel (2021). Foliar sprayed green zinc oxide nanoparticles mitigate drought-induced oxidative stress in tomato. *Plants*, 10 (11): 2400.
- Farghaly, F.A., H.K. Salam, A.M. Hamada, A.A. and Radi (2021). The role of benzoic acid, gallic acid and salicylic acid in protecting tomato callus cells from excessive boron stress. *Scientia Horticulturae*, 278: 109867.
- Farooq, M., H. Bramley, J.A. Palta and K.H. Siddique (2011). Heat stress in wheat during reproductive and grain-filling phases. *Critical Reviews in Plant Sciences*, 30 (6): 491-507.
- Gordon, J., H. Kazemian and S. Rohani (2015). MIL-53 (Fe), MIL-101, and SBA-15 porous materials: potential platforms for drug delivery. *Materials Science and Engineering, C* 47: 172-179.
- Grieve, C. and S. Grattan (1983). Rapid assay for determination of water soluble quaternary ammonium compounds. *Plant and Soil*, 70: 303-307.
- Halder, T., M. Choudhary, H. Liu, Y. Chen, G. Yan and K.H. Siddique (2022). Wheat proteomics for abiotic stress tolerance and root system

- architecture: Current status and future prospects. *Proteomes*, 10 (2): 17.
- Hamada, A. and A. El-Enany (1994). Effect of NaCl salinity on growth, pigment and mineral element contents, and gas exchange of broad bean and pea plants. *Biologia Plantarum*, 36: 75-81.
- Hasanuzzaman, M., K. Nahar, M.M. Alam, R. Roychowdhury and M. Fujita (2013). Physiological, biochemical, and molecular mechanisms of heat stress tolerance in plants. *International Journal of Molecular Sciences*, 14 (5): 9643-9684.
- Heikal, Y.M., M.A. El-Esawi, E.M. El-Ballat, and H.M. Abdel-Aziz (2022). Applications of nanoparticles for mitigating salinity and drought stress in plants: An overview on the physiological, biochemical and molecular genetic aspects. *New Zealand Journal of Crop and Horticultural Science*, 51 (4): 1-31.
- Hendawey, M.H. and H.A. Kamel (2015). Distribution and bioaccumulation of radiocarbon (^{14}C) into biochemical components of wheat in relation to antioxidant system under saline stress conditions. *Journal of American Science*, 11 (10): 8-21.
- Hendawey, M., E.A. Raheem, H.A. Kamel, G. Allah and N.E. Mahmoud (2018). Assessment of the contribution of exogenous polyamines for water stress tolerance in faba bean. *Bioscience Research*, 15 (2): 956-966.
- Herrera-Becerra, R., J. Rius and C. Zorrilla (2010). Tannin biosynthesis of iron oxide nanoparticles. *Applied Physics*, A 100: 453-459.
- Jaccard, P. (1908). Nouvelles recherches sur la distribution florale. *Bulletin de la Societe Vaudoise des Sciences Naturelles*, 44: 223-270.
- Jackson, M. (1958). In: 'Soil Chemical Analysis'. Constable and Co. Ltd., London.
- Khan, I., Saeed, K. and I. Khan (2019). Nanoparticles: Properties, applications and toxicities. *Arabian Journal of Chemistry*, 12 (7): 908-931.
- Kidane, Y.G., C. Mancini, D.K. Mengistu, E. Frascaroli, C. Fadda and M. Pè ME, Dell'Acqua (2017). Genome wide association study to identify the genetic base of smallholder farmer preferences of durum wheat traits. *Frontiers in Plant Science*, 8: 1230.
- Lu, Y., R. Li, R. Wang, X. Wang, W. Zheng, Q. Sun, S. Tong, S. Dai and S. Xu (2017). Comparative proteomic analysis of flag leaves reveals new insight into wheat heat adaptation. *Frontiers in Plant Science*, 8: 1086.
- Mahdi, A.A., N.E. Mahmoud and R.M. Abdelhameed (2021). The effect of incorporated *Aloe vera* extracts onto zeolitic imidazolate framework on physiological, biochemical, and molecular behavior of quinoa (*Chenopodium quinoa* Willd.) genotype under saline conditions. *Journal of Soil Science and Plant Nutrition*, 22 (5): 1-18.

- Mahmoud, N.E. and R.M. Abdelhameed (2021). Superiority of modified graphene oxide for enhancing the growth, yield, and antioxidant potential of pearl millet (*Pennisetum glaucum* L.) under salt stress. *Plant Stress*, 2: 100025.
- Mahmoud, N.E. and R.M. Abdelhameed (2022). Postsynthetic modification of ti-based metal–organic frameworks with polyamines and its behavior on biochemical constituents of *Sesamum indicum* L. under heat stress conditions. *ACS Agricultural Science and Technology*, 2 (5): 1023-1041.
- Mahmoud, N.E. and R.M. Abdelhameed (2023). Use of titanium dioxide doped multi-wall carbon nanotubes as promoter for the growth, endogenous indices of *Sesamum indicum* L. under heat stress conditions. *Plant Physiology and Biochemistry*, 201: 107844.
- Mahmoud, L.A., R.A. Dos Reis, X.Chen, V.P.Ting and S. Nayak (2022a). Metal-organic frameworks as potential agents for extraction and delivery of pesticides and agrochemicals. *ACS omega* 7 (50): 45910-45934.
- Mahmoud, N.E., A. Hassan and R.M. Abdelhameed (2022b). Microwave-assisted functionalization of graphene oxide with amino acid behaviour on the chemical constituents and specific molecular pathways of pearl millet grains under saline conditions. *Plant Nano Biology*, 2: 100020.
- Maity, A., N. Natarajan, D. Vijay, R. Srinivasan, M. Pastor and D.R. Malaviya (2018). Influence of metal nanoparticles (NPs) on germination and yield of oat (*Avena sativa*) and berseem (*Trifolium alexandrinum*). *Proceedings of the National Academy of Sciences, India Section B: Biological Sciences*, 88: 595-607.
- Mittal, D., G. Kaur, P. Singh, K. Yadav and S.A. Ali (2020). Nanoparticle-based sustainable agriculture and food science: Recent advances and future outlook. *Frontiers in Nanotechnology*, 2: 579954.
- Mittler, R. (2002). Oxidative stress, antioxidants and stress tolerance. *Trends in Plant Science*, 7 (9): 405-410.
- Modrow, A., D. Zargarani, R. Herges and N. Stock (2012). Introducing a photo-switchable azo-functionality inside Cr-MIL-101-NH₂ by covalent post-synthetic modification. *Dalton Transactions*, 41 (28): 8690-8696.
- Mondal, S., R. Singh, J. Crossa, J. Huerta-Espino, I. Sharma, R. Chatrath, G. Singh, V. Sohu, G. Mavi and V. Sukuru (2013). Earliness in wheat: a key to adaptation under terminal and continual high temperature stress in South Asia. *Field Crops Research*, 151: 19-26.
- Mueller, B., M. Hauser, C. Iles, R.H. Rimi, F.W. Zwieters and H. Wan (2015). Lengthening of the growing season in wheat and maize producing regions. *Weather and Climate Extremes*, 9: 47-56.

- Nakai, J. (2018). Food and Agriculture Organization of the United Nations and the sustainable development goals. *Sustainable Development*, 22: 1-450.
- Narayanan, S., P. Prasad, A. Fritz, D. Boyle and B. Gill (2015). Impact of high night-time and high daytime temperature stress on winter wheat. *Journal of Agronomy and Crop Science*, 201 (3): 206-218.
- Nazir, M., A. Bano, F. Ullah, S. Khan and N. Khan (2021). Physiological evaluation of wheat (*Triticum aestivum* L.) genotypes at pre-anthesis stage under heat stress conditions. *American Journal of Plant Sciences*, 12 (12): 1780-1790.
- Rasheed, A., H. Li, M.M. Tahir, A. Mahmood, M. Nawaz, A.N. Shah, M.T. Aslam, S. Negm, M. Moustafa and M.U. Hassan (2022). The role of nanoparticles in plant biochemical, physiological, and molecular responses under drought stress: A review. *Frontiers in Plant Science*, 13: 976179.
- Riaz-ud-Din, M., N. Ahmad, M. Hussain and A.U. Rehman (2010). Effect of temperature on development and grain formation in spring wheat. *Pakistan Journal of Botany*, 42 (2): 899-906.
- Rojas, S., A. Rodríguez-Diéguez and P. Horcajada (2022). Metal-organic frameworks in agriculture. *ACS Applied Materials and Interfaces*, 14 (15): 16983-17007.
- Semida, W.M., A. Abdelkhalik, G.F. Mohamed, T.A. Abd El-Mageed, S.A. Abd El-Mageed, M.M. Rady and E.F. Ali (2021). Foliar application of zinc oxide nanoparticles promotes drought stress tolerance in eggplant (*Solanum melongena* L.). *Plants*, 10 (2): 421.
- Shabala, S. and T. Cuin (2006). In: 'Osmoregulation Versus Osmoprotection: Re-evaluating the Role of Compatible Solutes'. University of Tasmania. Available online at: <https://hdl.handle.net/102.100.100/536694>
- Sharma, I., B. Tyagi, G. Singh, K. Venkatesh and O. Gupta (2015). Enhancing wheat production-A global perspective. *Indian Journal of Agricultural Sciences*, 85 (1): 3-13.
- Steel, R.G. and J.H. Torrie (1980). In: 'Principles and Procedures of Statistics'. McGraw-hill book Co. Inc., New York, 481 p.
- Sutulienė, R., L. Ragelienė, G. Samuolienė, A. Brazaitytė, M. Urbutis and J. Miliauskienė (2021). The response of antioxidant system of drought-stressed green pea (*Pisum sativum* L.) affected by watering and foliar spray with silica nanoparticles. *Horticulturae*, 8 (1): 35.
- Tan, X., S.Wang and N. Han (2022). Metal organic frameworks derived functional materials for energy and environment related sustainable applications. *Chemosphere*, 313: 137330.
- Ullah, A., A. Bano and N. Khan (2021). Climate change and salinity effects on crops and chemical communication between plants and plant growth-promoting microorganisms under stress. *Frontiers in Sustainable Food Systems*, 5: 618092.

- Usman, M., M. Farooq, A. Wakeel, A. Nawaz, S.A. Cheema, H. ur Rehman, I. Ashraf and M. Sanaullah (2020). Nanotechnology in agriculture: Current status, challenges and future opportunities. *Science of the Total Environment*, 721: 137778.
- Venkateswarlu, S., Y.S. Rao, T. Balaji, B. Prathima and N. Jyothi (2013). Biogenic synthesis of Fe₃O₄ magnetic nanoparticles using plantain peel extract. *Materials Letters*, 100: 241-244.
- Vu, T.A., G.H. Le, C.D. Dao, L.Q. Dang, K.T. Nguyen, P.T. Dang, H.T. Tran, Q.T. Duong, T.V. Nguyen and G.D. Lee (2014). Isomorphous substitution of Cr by Fe in MIL-101 framework and its application as a novel heterogeneous photo-Fenton catalyst for reactive dye degradation. *Rsc Advances*, 4 (78): 41185-41194.
- Wang, D. and Z. Li (2015). Bi-functional NH₂-MIL-101 (Fe) for one-pot tandem photo-oxidation/Knoevenagel condensation between aromatic alcohols and active methylene compounds. *Catalysis Science and Technology*, 5 (3): 1623-1628.
- Wang, X., B.S. Dinler, M. Vignjevic, S. Jacobsen and B. Wollenweber (2015). Physiological and proteome studies of responses to heat stress during grain filling in contrasting wheat cultivars. *Plant Science*, 230: 33-50.
- Waters, E.R., G.J. Lee and E. Vierling (1996). Evolution, structure and function of the small heat shock proteins in plants. *Journal of Experimental Botany*, 47 (3): 325-338.
- Wettstein, D. (1957). Chlorophyll letale and der sub mikroskopische for mwechsel der plastiden Exp. *Cell Research*, 12: 427-506.
- Weydert, C.J. and J.J. Cullen (2010). Measurement of superoxide dismutase, catalase and glutathione peroxidase in cultured cells and tissue. *Nature Protocols*, 5 (1): 51-66.
- Worthington, K. (2011). In: 'Worthington Enzyme Manual'. Worthington Biochemical Corporation. Lakewood, New York.
- Yang, L., K.-S. Wen, X. Ruan, Y.-X. Zhao, F. Wei and Q. Wang (2018). Response of plant secondary metabolites to environmental factors. *Molecules*, 23 (4): 762.
- Yildiztugay, E., C. Ozfidan-Konakci and M. Kucukoduk (2017). Improvement of cold stress resistance via free radical scavenging ability and promoted water status and photosynthetic capacity of gallic acid in soybean leaves. *Journal of Soil Science and Plant Nutrition*, 17 (2): 366-384.
- Yuan, Z., Y. Ye, F. Gao, H. Yuan, M. Lan, K. Lou and W. Wang (2013). Chitosan-graft- β -cyclodextrin nanoparticles as a carrier for controlled drug release. *International Journal of Pharmaceutics*, 446 (1-2): 191-198.
- Ze, Y., C. Liu, L. Wang, M. Hong and F. Hong (2011). The regulation of TiO₂ nanoparticles on the expression of light-harvesting complex II and

photosynthesis of chloroplasts of *Arabidopsis thaliana*. *Biological Trace Element Research*, 143: 1131-1141.

Zhang, Z., X. Li, B. Liu, Q. Zhao and G. Chen (2016). Hexagonal microspindle of NH₂-MIL-101 (Fe) metal–organic frameworks with visible-light-induced photocatalytic activity for the degradation of toluene. *RSC Advances*, 6 (6): 4289-4295.

تقييم الأثر العضوية النانوية لمعدن الحديد وحمض الجالنيك لتحمل الإجهاد الحراري في القمح بالوادي الجديد

نورا إبراهيم محمود

وحدة الكيمياء الحيوية، قسم الأصول الوراثية، مركز بحوث الصحراء، القاهرة، مصر

تم تنفيذ التجربة الحقلية بمحطة التجارب الزراعية لمركز بحوث الصحراء بمحافظة الوادي الجديد خلال موسمي ٢٠٢٢-٢٠٢٣، وذلك لتقييم مساهمة الأثر العضوية النانوية لمعدن الحديد وحمض الجالنيك في تحمل الإجهاد الحراري لصنفين من القمح (جيزة ١٧١ وجميزة ١٢). وتم تخليق الأثر العضوية النانوية لمعدن الحديد، ومن خلال عمليات التنشيط المختلفة واستخدام درجات حرارة مرتفعة تم إدخال وربط حمض الجالنيك بداخل الأثر العضوية النانوية. كما تم التأكد من تخليقها ونقاوتها بتوصيفها باستخدام أجهزة FTIR، XRD، HR-SEM. وقد أدت المعاملة بالأثر العضوية النانوية لمعدن الحديد والمرتبطة مع حامض الجالنيك وبخاصة المعاملة FeM4 لتخفيف التأثيرات السلبية للإجهاد الحراري على المنتجات الأيضية لنباتات القمح، كما أدت للمحافظة عليها من التأثيرات الضارة، وكان ذلك متوافقاً مع النمو والمحصول. وقد كان للمعاملة بـ FeM4 أفضل الأثر في تحسين إنتاجية محصول القمح بمقدار ٤.٣ و ٥.٤ مرة لصنفي جيزة ١٧١ وجميزة ١٢، على التوالي. كما وجد أن زيادة بعض المكونات الكيميائية وانخفاض البعض الآخر كان له دور في تخفيف التأثيرات السلبية الضارة للإجهاد الحراري على عمليات التمثيل الغذائي. فقد أدت المعاملة بـ FeM4 إلى زيادة محتوى أصباغ التمثيل الضوئي، وخاصة كلوروفيل (أ) بمقدار ١.٥٥ مرة، وكلوروفيل (ب) بمقدار ١.٤٢ مرة، وانخفاض محتوى البرولين بنسبة ٥٩٪ والجليسين ببيتان بنسبة ٢٣٪ مقارنةً بالكنترول. كما أدت المعاملة السابقة إلى زيادة نشاط إنزيمي البيروكسيداز superoxide dismutase في كلا صنفي القمح. أما على المستوى الجزيئي (تقنية ISSR) فقد أظهرت النتائج أن معاملة صنف القمح بالأثر العضوية النانوية لمعدن الحديد وحمض الجالنيك لم تؤدي إلى أي تغييرات ملحوظة في المادة الوراثية لنباتات القمح. ويمكن القول بأن تطبيق هذه التوصيات في المناطق الصحراوية الجديدة والمعرضة لظروف الإجهاد الحراري يمكن أن تلعب دوراً هاماً في زيادة إنتاجية محصول القمح (وخاصة جيزة ١٧١)، مما يساهم في تقليص الفجوة الغذائية للقمح في مصر.